A Biorobotic Flapping Fin for Propulsion and Maneuvering

James L. Tangorra, Member IEEE, George V. Lauder, Peter G. Madden, Rajat Mittal, Meliha Bozkurttas, Ian W. Hunter

***Abstract*—A series of biorobotic fins has been developed based on the pectoral fin of the bluegill sunfish. These robotic fins model physical properties of the biological fin, and execute kinematics derived from sunfish motions that were identified to be most responsible for thrust. When the physical properties of the robotic fin are tuned appropriately to operating conditions, the robotic fin, like the sunfish, produces positive thrust throughout the entire fin beat. Due to having many degrees of freedom, these fins can be used to generate and control forces for propulsion and maneuvering.**

I. Introduction

A robotic fin based on the pectoral fin of the bluegill sunfish has been developed. The fin is able to produce positive thrust throughout the entire fin beat, and can be made to produce and direct a wide range of forces appropriate for the propulsion and maneuvering of AUVs. The fin's design is the result of the analysis of the anatomy, mechanical properties, and kinematics of the biological fin, experimental and computational studies of the fin's hydrodynamics and forces, and an effort to identify and replicate in robotics the aspects of the fin's properties and kinematics that are most important to the production of propulsive forces.

The kinematics of many fish pectoral fins are often likened to those of bird or insect wings during flight in that the fins are flapped up and down [1,2]. However, the motion used by many bony fish – such as sunfish, perch, and fundulus – at low propulsion speeds and while executing maneuvers is actually quite different. Rather than being flapped up and down so that there is a leading and trailing edge like on a wing, the sunfish pectoral fin, for example, is swept forward and cupped about its spanwise axis such that the fin presents both an upper (dorsal) and lower (ventral) leading edge to the oncoming flow [3]. These kinematics are not described well by flapping wing or rowing analogies [2], and create very different hydrodynamics and forces. An important difference is that the sunfish pectoral fin is able to produce thrust throughout the entire fin beat, whereas fins that are flapped up and down tend to produce drag during a portion of the fin beat cycle [4,5,6]. This lack of drag is potentially very beneficial for propulsive efficiency and for creating smooth, continuous propulsive forces with flapping propulsors.

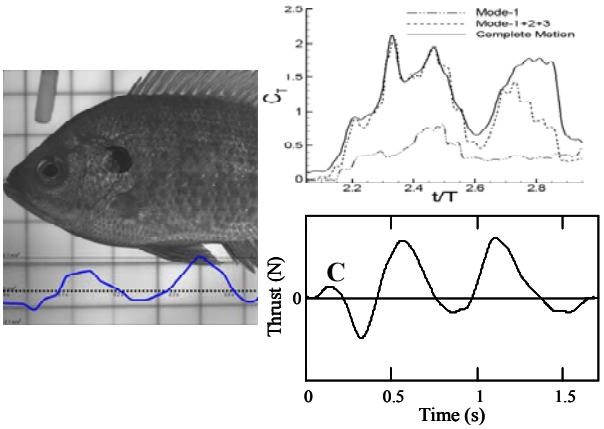

Figure 1. Acceleration of sunfish (A), CFD prediction of thrust coefficient (B), and thrust from the first generation biorobotic pectoral fin conducting a motion dominated by the cupping mode (C).

The development of a first generation biorobotic pectoral fin that produced motions which approximated those of a sunfish pectoral fin was reported recently [3,7]. The complex motions of the sunfish pectoral fin were decomposed using proper orthogonal decomposition (POD) into a small set of orthogonal modes [8,9], and the robotic fins were designed to recreate the four most energetic modes - sweep, curl, expansion, and cupping. The effect that each mode, and combinations of modes, had on fin forces was investigated experimentally and numerically. In general, fin motions that were dominated by a sweep of the fin into the flow produced drag during the outstroke (abduction) and thrust during the instroke (adduction). However, positive thrust could be created during the fin's outstroke when the fin's motion was dominated by the cupping and uncupping of the fin about its spanwise axis, and the sweep of the fin into the flow was limited in velocity and angular excursion. The resultant thrust forces exhibited two peaks, one during the cupping and one during the uncupping of the fin, and the pattern was consistent with accelerations measured for a sunfish when swimming exclusively with the pectoral fins and with CFD predictions of the forces generated during the outstroke of a fin movement that included cupping and sweep (Figure 1).

These results prompted the development of a second generation biorobotic fin, which will be discussed in this

Manuscript received **September 13, 2007.** This work was supported in part by the Office of Naval Research MURI Grant N000140310897.

J. L. Tangorra is with Drexel University, Philadelphia. PA 19104 USA ((215) 895-2296, e-mail tangorra@coe.drexel.edu).

G. V. Lauder is with Harvard University, Cambridge MA 02139 USA (e-mail glauder@oeb.harvard.edu).

P. G. Madden was with Harvard University. He is now with Evergreen Technologies, Marlboro, MA

R. Mittal is with The George Washington University, Washington DC, USA (e-mail mittal@gwu.edu).

M. Bozkurttas was with The George Washington University. She is now with Exa Corp., Burlington MA 01803

I.W. Hunter is with Massachusetts Institute of Technology, Cambridge, MA 02139 USA (e-mail ihunter@mit.edu).

paper. These second generation fins were designed to replicate the kinematics of the base of the sunfish fin during a POD Mode-1 movement [10], and were used to investigate the effects of the cupping and sweep motions, and the passive fin flexibility on the production of thrust and lift forces. These fins had many degrees of freedom, and were, therefore, not restricted to mimicking the sunfish movement. Alternate, non-biologically based kinematic patterns were also explored in order to identify manners in which the robotic fin could be used to generate forces appropriate for the maneuvering of undersea vehicles.

II. Fin Design

The robotic fins used five flexible fin rays, of lengths approximately four times those of the sunfish, attached to hinges mounted in a curved, rigid base (Figure 2). The webbings of the fin were made from thin (0.30 and 0.44 mm) polyester (82%) and elastane (18%) weaves. The curvature of the rigid base, and the angles at which the hinges were set, caused the fin to cup about its spanwise axis as the fin rays were swept forward. Each fin ray was actuated individually by linear Lorentz force servomotors via a nylon tendon attached to the fin ray's lower structure. The linear servomotors were developed in house [12]. The rigid base and flexible fin rays were manufactured using stereolithography (3D Systems, Rock Hill, NC).

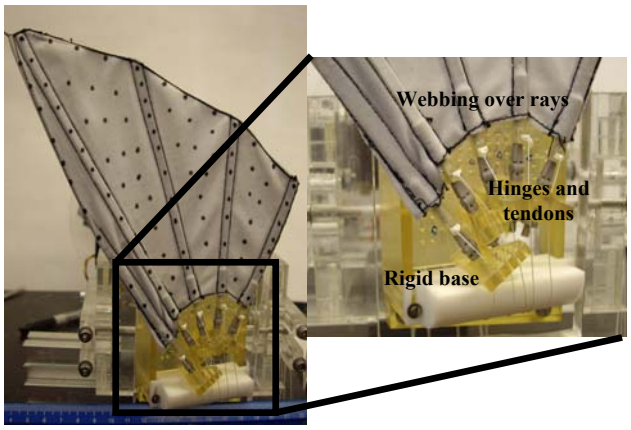

Figure 2. Biorobotic fin with detail of fin's rigid base.

Rigid base

The geometry of the fin's rigid base was designed by analyzing the movements of the five biological fin rays (1, 4, 7, 10, 14) that best defined the shape of the sunfish fin throughout Mode-1. The other nine fin rays are important to the fin's structure, but are located within areas of the fin where the shape was bounded by the five selected rays, and were omitted to simplify the design and analysis. The positions of 20 points along each of the fin rays were tracked through time and plotted in 3D. Near the base, the fin rays remained straight and had a trajectory that could be approximated as the rotation of a line segment in a plane, about a point external to the segment. Away from the base, the flexible rays bent and twisted and did not remain aligned with the lower portion of the fin ray. Lines were fitted to the three points nearest each fin ray's base at 20 time increments, centers of rotation were found, and the fin's rigid base was designed so that the hinge point of each fin ray would be located at this rotational point. The trajectory of each fin ray during Mode-1 was mapped in time, and was fitted using a five term Fourier series. These time functions were used to drive the actuators so that velocity profile of each robotic fin ray was correct for the Mode-1 movement.

Fin rays

The robotic fin rays were constructed with flexural rigidities (EI) proportional to the passive flexural rigidities of the sunfish fin rays. This was done so that the flexibility of the robotic fins would vary across the chord and from root to tip in a manner similar to that of the fish fin. The structure and flexural stiffness of several biological fin rays had been analyzed (Madden and Lauder, unpublished data), so the area moment of inertia (I) and modulus of elasticity (E) was known at several points along the fin rays. The flexural rigidity of the biological fin rays is due to passive elastic properties of bone and collaganeous intra-ray material, and, as well, to active modulation of the fin rays by the fish; but for simplicity the robotic fin rays modeled only the passive properties. Active modulation of fin ray shape and stiffness had been investigated previously [3] so its effect and the advantages it provided were already understood.

Because the robotic fins were larger than the fish fins, and were to be operated at different flapping speeds and flow rates, the flexural rigidity of each fin ray had to be scaled so that the robotic fin would behave and bend in a manner similar to the fish fin. A first order estimate of the bending of the fin rays was made using the Euler-Bernoulli beam equation, modeling the biological fin rays as cantilevers, and assuming that the bending forces acting on the fin were caused by drag on the fin as it was flapped through the water. A scaling rule was calculated that showed that each of the five ray robotic fins would bend by the same fraction of length as the fourteen biological rays when the robotic fins' flexural rigidities were scaled with the square of the fin's flapping frequency (f) and with the length of the ray to the sixth power. Based on a range of measurements taken from several biological fin rays, the flexural rigidities desired for the robotic fin rays were estimated to be approximately 500 to 1000 times that for the corresponding fish fin rays.

Fin rays were built with rectangular cross sections that either tapered in thickness and width from the base to the tip of the fin ray (Figure 3), or that remained uniform along the fin ray's length. The tapered cross section is similar to the geometry of the biological fin rays [12], and the dimensions were selected by fitting via least squares the flexural rigidities of the robotic rays to those of the biological rays scaled to the desired level. The dimensions of the rays with the uniform rectangular cross sections were selected using finite element models (Nastran, MSC Corp., Santa Ana, CA) so that the rays would bend by the same amount at the tip as the tapered rays under similar loading conditions. Due to the different geometries, the tapered and uniform fin rays

exhibited different curvatures when loaded. The uniform rays were predicted to bend most near the base, where the ray was anchored, and to be rather straight near the tip. In contrast, the tapered rays, which were thicker at the base and thinner at the tip than the uniform rays, were predicted to have a more uniform curvature along their length.

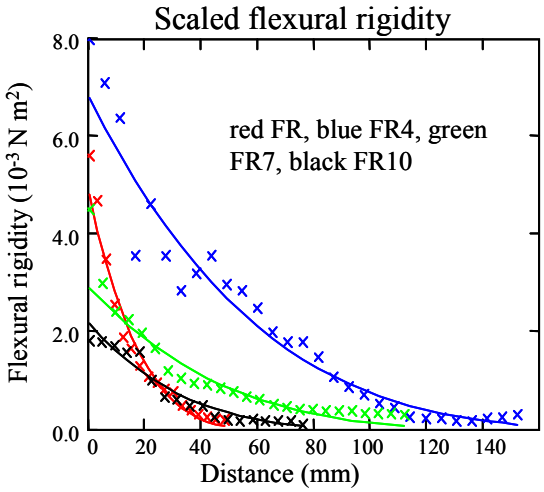

Figure 3. The flexural rigidity of four fin rays (solid) with rectangular cross sections that tapered in height and width fitted to the flexural rigidity of the actual fin rays (x), scaled 500 times.

III. Experimentation

The kinematics and forces of nine fins with flexural rigidities of 500, 600, 1000, and 5000 times that of the biological fish fin rays were evaluated. The most rigid fin was very stiff and did not bend visually when moved through the water. It was used to investigate if the kinematics of the cupping and sweep motions alone would be sufficient to create thrust during the outstroke, or if it was necessary to have the motion coupled to a flexible fin. It had been shown previously that flexibility alone was not sufficient to cause a flapping fin to produce thrust during the outstroke [3]. One of the fins also had its webbing resized such that it became taught when the fin was approximately ¾ uncapped.

The fins were mounted to an air bearing sled and were lowered into a flow tank [3]. Forces were measured simultaneously along the thrust (*anterior-posterior*) and the lift (*dorso-ventral*) axes. Fins were tested at flapping frequencies of 0.30, 0.50, 0.65, 1.00, 1.35, 1.65 Hz, and 2.00 Hz and at flow rates of 0, 90, 180, 270, and 360 mm/s. These operating conditions corresponded to Strouhal numbers ranging from 0.14 to 3.78, and infinite when flow rate was zero. This range spanned and exceeded the Strouhal numbers (St) that were used in the experimental testing and CFD analyses of the biological fins.

The biorobotic fins were also made to operate using several kinematic patterns that were not based on those of Mode-1. For example, a movement was used which was similar to a flapping motion where the dorsal fin ray served as the leading edge and the most ventral fin ray served as the trailing edge. Rather than activating the fin rays synchronously so that the fin cupped, the dorsal ray was actuated first and then followed by the more ventral rays. Each ray lagged its preceding ray by 30 degrees such that the most ventral ray lagged the most dorsal ray by 120 degrees.

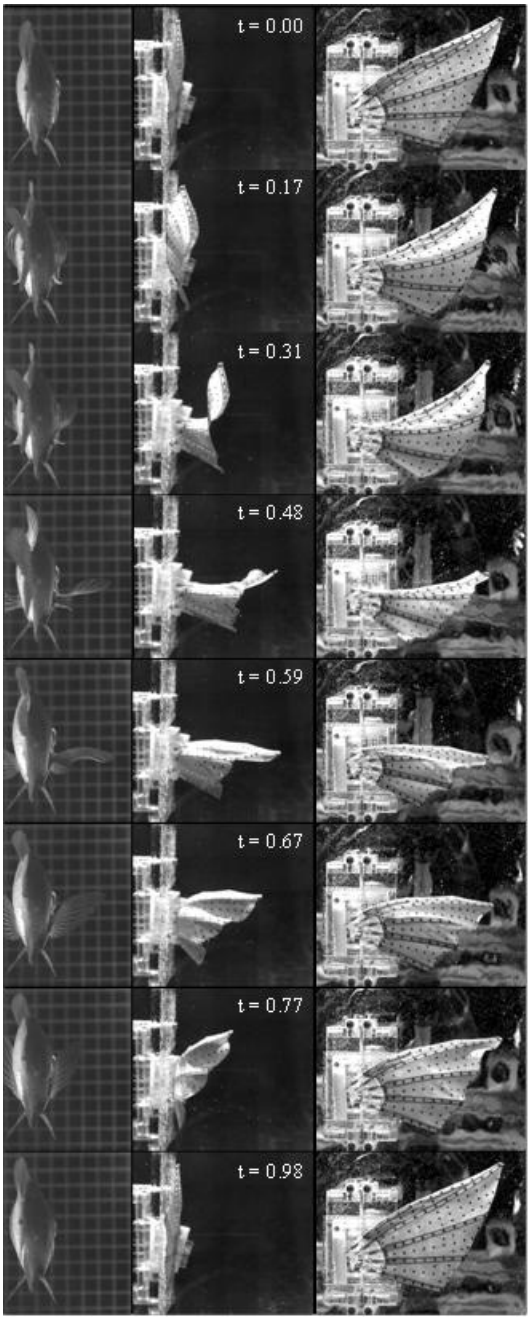

Figure 4. Posterior view of sunfish during steady swimming (left). Posterior (center) and lateral (right) views of a flexible robotic fin (flexural rigidity 600×) executing Mode-1 motions at St = 1.89. The fin's outstroke occurs from t = 0.00 s to approximately t = 0.48 s. In the lateral view, the robotic fin is moving towards the reader during the outstroke and into the page during the instroke.

High speed, high resolution video was taken of the fins as they were tested to enable the evaluation of fin kinematics and simulation of the fin movements in CFD. Cameras

(Photron USA, Inc. San Diego CA) were arranged to capture the ventral, lateral, and posterior views of the fin, and were operated at 250 frames per second.

IV. Results

Fin Movements

The movements of the flexible robotic fins were strikingly similar to those of the sunfish fin (Figure 4). The fins produced the complex bending and 3D curvatures exhibited by the fish fin. The lower portions of the fin rays remained straight throughout the fin beat, and the more distal portions were bent and curved by normal forces from the fluid and lateral forces from the webbing between the rays. As for the fish, the distal end of the robotic fin bent back as the fin moved into the flow such that the forward surface of the fin's webbing faced backwards (Figure 4, t = 0.17 s, 0.31 s, 0.42 s). The top of the fin moved forward and down, such that by the end of the outstroke the upper half of the fin's webbing was nearly horizontal (Figure 4, t = 0.48 s). The distal end of the fin continued to move forward into the flow after the base of the fin had begun the instroke, and as the fin came back during the instroke, the fin opened and the webbing expanded. In contrast to the fish fin webbing, which remained smooth and taught throughout the fin beat, the webbing of the robotic fin was looser, and at times folded upon itself.

The similarities between the robotic fin's movements and the biological fin's movements support strongly the importance of the fin's passive flexibility in creating an appropriate fluid-structure interaction and fin movement. The robotic fins are actuated at their root to recreate the kinematics of POD Mode-1, which accounts for only 37% of the dynamics of the motion performed by the fish [3,9]. When executed by the stiffest of the robotic fins, the movement through the water did not look like the fish fin, nor did the fin produce positive thrust during the outstroke. The fin did execute the proper cupping and sweep motions at the base, but there was no bending of the fin nor was there an obvious dynamic fluid-fin interaction. In contrast, the dynamic interaction of the flexible fins with the water made the robotic fin move like a biological fin, and was what was necessary to produce thrust during the fin's outstroke.

Forces

Like the fins of the sunfish, the flexible robotic fins were able to produce thrust throughout the entire fin beat. Representative forces are shown in Figures 5 and 6. Two peaks of thrust occurred in every trial, with the peak magnitude and impulse imparted to the water being greater during the instroke than the outstroke. Thrust occurred during the transition period when the operating conditions were "correct". Based on a visual analysis of the robotic fin's motion, we suspect this occurred when fin stiffness, flapping frequency, and the speed of the water flow were tuned such that the fin "unbent" just as it ended its outstroke and with enough speed to accelerate the water aft of the fin to speeds greater than that of the free-stream flow. Lift forces (Figure 5, bottom) were correlated to the movement of the dorsal half of the fin. Lift occurred during the outstroke as the upper half of the fin was brought down and forward into the flow, and downward force (negative lift) occurred as the fin was brought back.

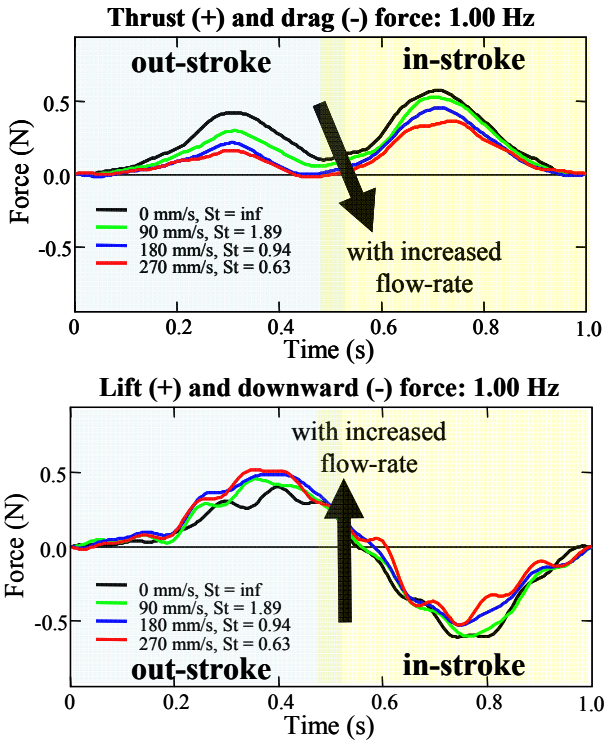

Figure 5. Fin forces at different flow rates. Thrust and drag (top), and dorsal (lift) and ventral (downward) forces produced by a cupping-fin (rigidity 1000×) when actuated at a rate of 1.00 Hz. Thrust is reduced, and lift is increased as flow speed rises.

The forces generated by each fin were dependent on the speed of the free-stream flow (U) and the fin's flapping frequency (f). The basic shapes of the force curves for a particular fin did not change considerably as U and f varied, but the magnitudes of the forces did. As the speed of the water increased, the thrust and drag curve was shifted downward towards drag, and the lift curve moved upwards for increased lift. When flow speed was high enough, drag was created at the end of the outstroke and throughout the transition to the instroke. Forces increased with increased flapping frequency (f), but only to a point. Thrust forces decreased when a fin's flapping frequency exceeded a certain frequency, usually around 1.00 Hz. For example, for the fin that produced the data in Figure 6, the magnitude of the thrust during the outstroke and instroke decreased after 1.30 Hz. It could be seen on the high speed video that the fin acted like a low pass system. At the higher frequencies tested, the distal end of the fin did not move through as large of a displacement as during the lower frequencies, despite the base of the fin rays being actuated through the same full movement. The smaller displacements of the distal end resulted in lower forces.

Effects of fin ray shape and stiffness

Fins with tapered fin rays produced consistently larger thrust forces than fins of similar stiffness with rays

that had the uniform, rectangular cross section (Figure 7). The difference was most pronounced during the outstroke. Fins with tapered rays were not wholly better during the instroke, but for fins of similar stiffness, tapered rays, in general, resulted in higher thrust forces. The lift forces were similar between fins with different fin ray cross sections.

Although the overall deflection of the fins was similar, it could be seen during the experimental trial, and from finite element simulation of the fin rays, that the tapered fin rays curved more near the tip than the uniform rectangular fin rays. It is believed that with the tapered rays, the distal end of the fin bent more as the fin moved into the flow. More of the fin's surface was therefore positioned to push water back and to produce force in the thrust direction (Figure 4, t = 0.17 to 0.42). The difference between the bending of the fins was subtle, but the result was consistent.

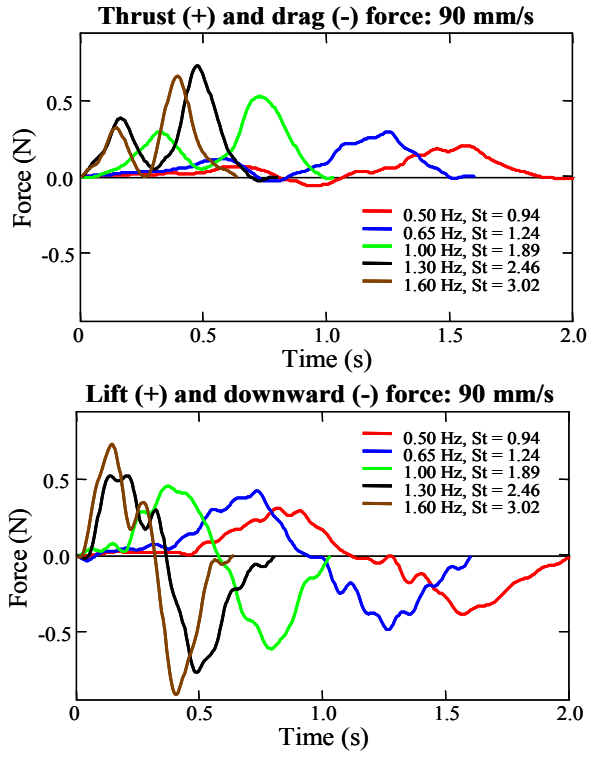

Figure 6. Fin forces at different flapping frequencies (rigidity 1000×). During both the outstroke and instroke, the maximum magnitude thrust occurred when flapping frequency was tuned appropriately to flow rate and fin flexibility.

Stiffness affected the magnitude of the forces, but no single stiffness was best for maximizing thrust force throughout a fin beat. It is apparent in Figures 5, 6, and 7 that a particular fin produced maximum forces throughout the fin beat at a specific flow speed and flapping frequency. However, for specific conditions (U and f), maximum forces were created at different portions of the fin beat by fins of different stiffness. For example, at 1.00 Hz and 90 mm/s, the maximum thrust during the outstroke was produced by the stiffest tapered fin (1000×), while maximum thrust during the instroke was created by a slightly more compliant fin (600×). This pattern held, with few exceptions, at flapping frequencies at, and above, 1.00 Hz for all flow rates, but was different at lower flapping frequencies. For example, when the flapping frequency was reduced to 0.65 Hz (U = 90 mm/s), the tapered fin with a stiffness of 500× produced the highest thrust during both the outstroke and instroke. Whereas fins with tapered fin rays (and therefore flexural rigidities that varied along the fin's span in a manner similar to that of the biological fin) consistently produced larger forces than fins with rays of a uniform flexural rigidity, fins with flexural rigidities that varied chordwise (in a manner like the biological fin) did not produce better forces than fins with fin rays that had the same root and the tip dimensions.

Alternative kinematic patterns

The forces, and predominant direction of the forces, produced by the robotic fin could be altered significantly by changing the pattern in which the fin rays were actuated. Although restricted to move within the paths defined by the Mode-1 movement, the fin rays, by virtue of being actuated individually, could be moved to create many different patterns by altering speed, displacement, and phase relations. For example, the equivalent of a flapping motion, where the fin has a clear leading and trailing edge, was created by moving the fin rays sequentially rather than synchronously. In these cases, the dominant force produced by the fin was along the lift axis, rather than thrust (Fig. 8).

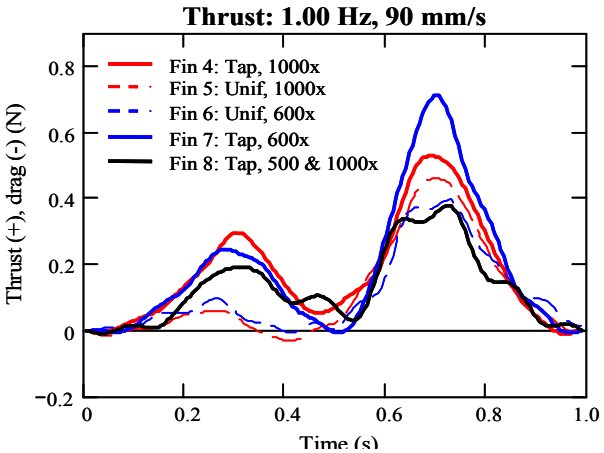

Figure 7. Thrust forces from fins with tapered (solid) and uniform (dashed) fin rays of similar overall compliance. Different fins, and therefore different fin ray compliance, produced maximum forces at different points in the fin beat.

V. Conclusions and Future Work

By learning from the sunfish, we have developed a biorobotic fin propulsor with characteristics that are advantageous for propelling and maneuvering AUVs. When operated at a frequency that tunes the fin's dynamics to flow conditions, the fins produce thrust throughout the fin beat, and lift forces of approximately the same magnitude as peak thrust. CFD analysis (Bozkurttas unpublished data) show similar magnitudes for the side forces. The lack of drag, and relatively low lift and side forces suggest that fins which employ the sunfish pectoral fin's cupping and sweep motion may be more efficient at low speeds than flapping based fins which produce drag, and also lift and side forces that are larger in magnitude than the propulsive forces. The many

degrees of freedom that are created by actuating the fin rays individually allows these fins to execute non-biologically based motion such as the dorsal lead (Figure 8) or one in which only the top half or bottom half of the fin is used to generate a lift or downward force. By controlling the speed, displacement, and phase relations between the fin rays, this fin design can control maneuvering forces throughout the 2D lift, thrust plane.

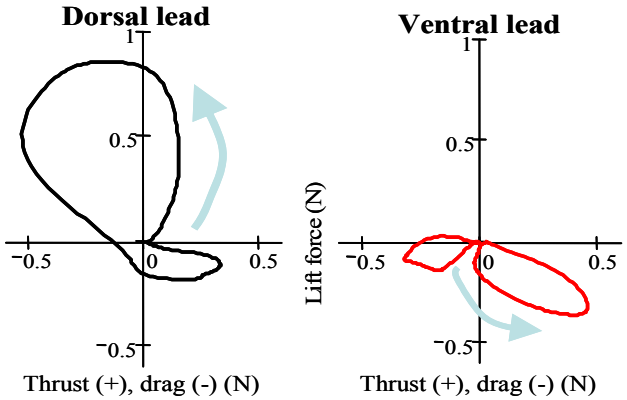

Figure 8. 2D forces from a 1.0 Hz "dorsal lead" (left) and a "ventral lead" flapping motion. Lift is on the vertical (+) axis and thrust is on the horizontal (+) axis. These motions are two of many non-biological patterns that can be used to alter the direction and magnitude of the fins forces.

Fin stiffness is key to the production of thrust forces, and our data suggest that active modulation of the fin ray stiffness should be employed to maximize fin forces. Individually, each fin produced maximum thrust when operated at a particular flapping frequency, often during both the instroke and outstroke (Figure 6). However, for a given set of conditions (flapping frequency and flow rate), no single fin produced the highest forces throughout the fin beat cycle (Figure 7). Maximum forces at different points in the fin beat came from fins of different stiffness. These results contrast previous results from experiments with flapping fins where increasing the stiffness of fin increased the magnitude of thrust during the instroke [3]. Therefore, there is not a simple relation between fin stiffness and fin force. The fin is clearly a dynamic structure with dynamics that are coupled to its fluid environment. The fin and the fluid need to be viewed and analyzed as a coupled system as we are doing in the CFD analysis. To maximize thrust and the impulse imparted to the water, it will likely be necessary to alter the fin's stiffness, and its dynamic interaction with the water, throughout the fin beat and as operating conditions change. As demonstrated in Tangorra et al. [3], this could be done by using a fin ray that undergoes a geometric change when actuators pull on its base. There is some evidence that the sunfish may do just this. Our studies of the fish have shown there to be co-contraction of the muscles at the base of the fin rays during steady swimming. Co-contraction would seem to increase the energy expended in a fin beat, which would not seem beneficial to the fish, but perhaps it is done to tune the fin's dynamics and optimize fin performance.

The shape of the fin rays – and therefore their resultant curvature and the dynamics of how they released stored energy when they unbend – had a great impact on force, particularly during the outstroke. Rays that, as in the sunfish, tapered from a thick base to a thin tip produced larger thrust forces than rays of similar stiffness with uniform cross sections. This outcome supports the assertion that a superficial modeling of a biological system is often insufficient. Biological systems have the details they do for good reason.

The results for these biorobotic fins are not completely consistent with results from a CFD analysis of the biological fin. The CFD analysis shows that the fish fin generates its greatest thrust near St = 0.5. However, for the biorobotic fins, maximum thrust, at every frequency, occurred when the flow rate was zero. This issue will be investigated by using digital particle image velocimetry (DPIV) to compare the hydrodynamics of the robotic fins to CFD simulations and DPIV of the actual fish.

We are currently conducting efficiency studies of these robotic fins and developing a final fin design that merges the aspects of our first two robotic fins which we have determined to be most important to the production and control of propulsion and maneuvering forces.

REFERENCES

[1] J.A. Walker and M. A. Westneat, "Labriform propulsion in fishes: kinematics of flapping aquatic flight in the bird wrasse, Gomphosus varius," J. Exp. Biol., vol 200, 1997, pp 1549-1569.

[2] J. A. Walker and M. A. Westneat, "Mechanical performance of aquatic rowing and flying", *Proc. R. Soc. Lond. B*, vol. 267, pp 1875-1881, 2000.

[3] J. Tangorra., S.N. Davidson, I.W. Hunter, P.G.Madden, G.V. Lauder, H. Dong, M. Bozkurttas, R. Mittal, "The development of a biologically inspired propulsor for unmanned underwater vehicles", IEEE J. Oceanic Eng. in press.

[4] A. Techet,, K. Lim, F. Hover, M. S. Triantafylou, "Hydrodynamic performance of a biologically inspired 3D Flapping foil", 14th International Symposium on Unmanned Untethered Submersible Technology, 2005, Durham, New Hampshire, USA.

[5] H. Dong,, R. Mittal, F.M. Najjar, "Wake Topology and Hydrodynamic Performance of Low Aspect-Ratio Flapping Foils," J. Fluid Mech., 566, 2006, pp.309-343.

[6] J. Palmisano, R. Ramamurti, K.J. Liu, J. Cohen, W. Sandberg, B. Ratna, "Design of a Biomimetic Controlled-Curvature Robotic Pectoral Fin", 2007 IEEE International Conference on Robotics and Auromation, Roma, Italy, pp 966-973

[7] G.V. Lauder, E.J. Anderson, J.L. Tangorra, P.G. Madden, "Fish biorobotics: kinematics and hydrodynamics of self-propulsion" J. Exp. Biol. 210, 2007, pp 2767-2780.

[8] M. Bozkurttas, H. Dong, R. Mittal, P. Madden, G.V. Lauder, "Hydrodynamic Performance of Deformable Fish Fins and Flapping Foils," *AIAA 2006-1392*, Reno, NV.

[9] M. Bozkurttas, "Hydrodynamic performance of fish pectoral fins with application to autonomous underwater vehicles". Ph.D. thesis, The George Washington University, Washington DC, 2007.

[10] M. Bozkurttas, H. Dong, R. Mittal, J. Tangorra, I. Hunter, G. Lauder, P. Madden, "CFD based Analysis and Design of Biomimetic Flexible Propulsors for Autonomous Underwater Vehicles". AIAA *2007-4213*, Miami, FL, June 2007

[11] N. Ball, "The Development of a High Power Density Linear Lorentz Force Actuator", Master's Thesis, Massachusetts Institute of Technology, Cambridge MA, 2007

[12] S. Alben, P.G. Madden, G.V. Lauder, G.V. "The mechanics of active fin-shape control in ray finned fishes", J. Roy. Soc. Interface, 4, 2007, pp 243-256